International Journal of
Nanoscience and Nanotechnology

Research Article 2025, Volume 21, Issue 3

Novel Method for Synthesis of Janus MXene Nanosheets by Masking Starch

Fateme Helmi, Mahdieh Yavari, Esmail Yaghoubi-Azbari, Mahdi Akbari, Mojtaba Shariaty-Niassar*

Received 19 July 2025
Accepted 5 September 2025

DOI: 10.22034/ijnn.2026.2066281.2683

International Journal of Nanoscience and Nanotechnology

Abstract

MXene represents a highly promising class of two-dimensional materials characterized by its layered structure; however, the interlayer van der Waals forces result in aggregation of these nanoparticles and limit their application. To address this challenge and enhance their stability and applicability, strategies such as composite formation and surface modification are utilized. Notably, transforming MXenes into Janus structures has emerged as an effective strategy to enhance functionality. Janus MXene nanosheets were synthesized via the Pickering emulsion method. In this method, one side of the MXene was masked with tapioca starch microspheres. Afterward, MXene was functionalized with dodecylamine (DDA), a hydrophobic agent. Subsequently, the starch template was removed from the MXene surface via thermal cycling (heat and sonication). Then, Janus MXene nanosheets with an asymmetric structure were synthesized. This study introduces a novel and cost-effective method for synthesizing hydrophilic/hydrophobic Janus MXene nanosheets. FTIR, Raman, XRD, and FESEM analyses collectively confirm the amphiphilic behavior and the two-dimensional structure of the synthesized Janus MXene nanosheets. This synthesis method is viable and economical for the production of Janus MXenes.

Keywords: Two-dimensional nanomaterials, Amphiphilic nanosheets, MXene, Synthesis of Janus NPs, Janus MXene

How to cite this article

Helmi F, Yavari M, Yaghoubi-Azbari E, Akbari M, Shariaty-Niassar M. Novel Method for Synthesis of Janus MXene Nanosheets by Masking Starch. Int. J. Nanosci. Nanotechnol., 2025;3: 149-156. DOI: 10.22034/ijnn.2026.2066281.2683

1. Introduction

Two-dimensional nanoparticles possess mechanical strength, a high surface area, and tunability, making them suitable for various applications [1]. Among these, MXenes, a recently discovered family of 2D materials, have high electrical conductivity, hydrophilic nature, and remarkable surface area [2], which makes them ideal for energy storage [3], catalysis [4], and sensor [5] applications. To enhance their stability and processability, MXenes are modified via surface functionalization [6] or by creating a composite [7]. Among these strategies is a transformation into Janus structures [8]. Janus materials (named after the dual-faced Roman god Janus) have attracted significant interest due to their asymmetrically functionalized surfaces, which enable new levels of interfacial properties and multifunctionality, creating emerging opportunities in nanotechnology [9]. They can exist in several geometries, such as spheres, cylinders, disks, and bowls [10]. Janus nanoparticles (JNPs) are a class of heterogeneous materials consisting of two distinct sides, each with unique chemical or physical properties; one side can be hydrophilic (water-attracting), while the other can be hydrophobic (water-repelling) [11]. Janus nanoparticles, owing to their amphiphilic nature, have immense applications in drug delivery [12], catalysis [13], adsorption [14], oil/water separation [15], biomedical imaging and therapy [16,17], etc.

Chen M. et al. [18] created Janus MXene ink with asymmetric surface chemistry by grafting polystyrene onto MXene nanosheets, making them hydrophilic on one side and hydrophobic on the other. This modification produces additive-free organic inks with excellent dispersibility in polar and nonpolar solvents, resolving substrate-compatibility issues. The Janus nanosheets extend ink shelf life, retain 90% of solids in toluene after a month by reducing oxidation, and enable uniform coating on various substrates. These coatings exhibit enhanced photothermal properties, chemical stability, and EMI shielding performance. Akbari et al. [19] used Janus GO nanosheets to improve water treatment membranes. The dual-surface Janus structure enhanced nanosheet dispersion into polymer matrix, making Janus polysulfone (PSf) membranes more hydrophilic with higher water flux. membranes containing 1 wt.% Janus GO also showed better antifouling performance. This work highlights Janus GO's potential to improve membrane performance by reducing fouling and hydrophobicity. Zhao et al. [20]

Transport Phenomena & Nanotech. Lab (TPNT), School of Chemical Engineering, College of Engineering, University of Tehran, Tehran, Iran

E-mail: mshariat@ut.ac.ir

developed Janus MXene nanosheets (JMNs) by grafting polystyrene onto one side of the MXene, yielding an amphiphilic structure with a hydrophobic polymer and hydrophilic MXene surfaces. This asymmetry enables JMNs to act as solid surfactants, facilitating spontaneous assembly at water-oil interfaces, thereby reducing interfacial tension and stabilizing emulsions. Their Janus architecture ensures excellent dispersibility in both aqueous and organic solutions and enables scalable macroscopic assembly through interfacial organization. Chen X. et al. [21] prepared SSK1@PDA/CaP@CIP Janus nanoparticles (JNPs) for Pseudomonas aeruginosa pneumonia. The JNPs combined a hydrophobic SSK1 (anti-inflammatory prodrug) with a hydrophilic ciprofloxacin (CIP, antibiotic), providing anti-inflammatory and antibacterial/biofilm-eradication effects. In vivo tests showed effective treatment, good biocompatibility, and no significant organ damage. Results suggest JNPs are as a novel therapy for bacterial pneumonia.

Janus nanosheets have many scientific applications but, are difficult to synthesize due to their asymmetric structure. Ensuring material compatibility is challenging, as dissimilar materials can cause phase segregation or unwanted deposition due to surface energy differences, requiring precise control [23-25]. Techniques like chemical vapor deposition (CVD) [26] and atomic layer deposition (ALD) [27] are costly and complex, limiting scalability and adoption [28,29]. Synthesizing Janus MXene nanosheets is further complicated by MXenes' layered structure [30] and van der Waals forces [31,32], which promote aggregation and reduce dispersion and performance. So far, only two studies have reported the synthesis of Janus MXene using a masking approach, and both employed essentially the same fabrication strategy [18-20]. In these methods, polystyrene was used as a hydrophobic masking agent, which requires the prior synthesis of polystyrene microspheres and subsequent deposition of MXene sheets onto their surfaces. The preparation of these microspheres is time-consuming and technically demanding. Moreover, the harsh thermal treatment required to decompose the polystyrene spherical template led to partial oxidation of titanium carbide MXene into titanium oxide, which reduced its efficiency [18-20].

This work reports the first synthesis of Janus MXene nanosheets using a starch-based masking approach, a new strategy. The synthesis began by etching the Titanium Aluminum Carbide (Ti_3AlC_2) precursor in hydrofluoric acid (HF). MXene layers were then separated by dispersion in dimethyl sulfoxide (DMSO). A starch-based coating was applied to selectively mask one side of the MXene nanosheets. Due to MXene's hydrophilicity, the exposed surface was modified with dodecylamine (DDA) to make it hydrophobic, forming an asymmetric Janus structure. In this synthesis method, tapioca starch microspheres are used as the coating agent. They have a regular spherical structure and are inexpensive and readily available. The advantage of this synthesis method over those in [18] and [20] is that it does not require the synthesis of a coating agent. The thermal cycle used to separate Janus MXene from starch microspheres is very mild and does not destroy the maxin structure. This makes this method a convenient and inexpensive approach for the synthesis of Janus MXene. Successful functionalization was confirmed by Raman spectroscopy, X-ray diffraction (XRD), and Fourier-transform infrared spectroscopy (FTIR), showing MXene and DDA functionalities. Field-emission scanning electron microscopy (FESEM) images revealed the two-dimensional morphology, confirming proper preparation and structural integrity.

2. Materials and methods

2.1. Materials

The materials used for nanoparticle fabrication include: Titanium Aluminum Carbide powder (RedoxKala), Tapioca starch (Phoenix brand), hydrofluoric acid (HF, 40%; Merck), dimethyl sulfoxide (DMSO; Merck), isopropanol (99.8%; Merck), dodecylamine (DDA; Merck), and Chloroform (Merck). All solutions were prepared using triple-distilled (TD) water.

2.2. Characterization

To characterize the morphology of MXene nanosheets and Janus MXenes, a Field emission scanning electron microscopy (FE-SEM; TESCAN MIRA3) was used. Samples for FE-SEM were prepared by sonicating the suspension of MXene and Janus MXene in isopropanol, followed by drop-casting onto the substrate. Fourier transform infrared spectroscopy (FT-IR) was conducted using a Thermo Avatar spectrometer to characterize the functional groups in MXene and Janus MXene samples. The samples for this analysis were made into KBr pellets. Raman spectroscopy (BRUKER SENTERRA) with an excitation laser at 785 nm and a 200-3500 cm^{-1} range was used. The Philips X'Pert Pro was used to perform X-ray diffraction (XRD) with Cu radiation.

2.3. MXene preparation

$Ti_3C_2T_x$ MXene was obtained by etching the Ti_3AlC_2 powder in 10 mL of HF (40%) within a PTFE reactor (Figure 1). To remove the aluminum layer, the mixture was stirred for 24 h (room temperature) at 600 rpm. After etching, the MXene was washed with centrifugation at 3500 rpm for 5 min. The supernatant was collected, and the solid was washed with triple-distilled water until the pH of the wash solution was 5-6. The obtained MXene was dried under a vacuum at 75°C for 24 hours.

2.4. Janus MXene preparation

To synthesize a Janus MXene, MXene layers were initially separated by dispersing 40 mg of MXene in 80 mL of DMSO and stirring for 24 hours to allow DMSO intercalation. Centrifugation at 5000 rpm for 20 minutes separated the MXene particles from the solution. Then, 40 mL of DI water was added to the MXene, and the mixture was ultrasonicated. In parallel, 16 g of tapioca starch was suspended in 100 mL of DI water and stirred at 250 rpm for 2 hours to disperse starch microspheres. The MXene suspension was slowly added to the starch mixture and stirred for 6 hours at 250 rpm under an argon atmosphere, allowing MXene

to adsorb onto starch microspheres via hydrogen bonding. The starch microspheres were filtered and washed with water and isopropanol to remove free MXene. 120 mg of DDA was dispersed in 20 mL of isopropanol and mixed well before adding solution to the MXene/starch composite in 100 mL of isopropanol for functionalization. The DDA solution was stirred for 12 hours under an argon atmosphere at 250 rpm to coat the MXene layers. The starch/MXene/DDA mixture was washed with isopropanol to remove excess unreacted DDA. DDA-MXene-coated starch microspheres were dispersed in 50 mL of isopropanol and then subjected to thermal cycling at 40 °C to strip the DDA-MXene layers. A two-phase suspension formed: a dark phase of JMX nanosheets and a white phase of precipitated starch. The suspension was centrifuged at 2000 rpm to remove impurities, and the liquid containing JMX was collected by careful pouring. Finally, to confirm the Janus configuration and remove impurities (unreacted MXene and DDA), the as-synthesized JMX nanosheets were added to a decant of DI water (hydrophilic phase) and chloroform (hydrophobic phase). The successful synthesis was evidenced by JMX nanosheets at the liquid-liquid interface (Figure 2).

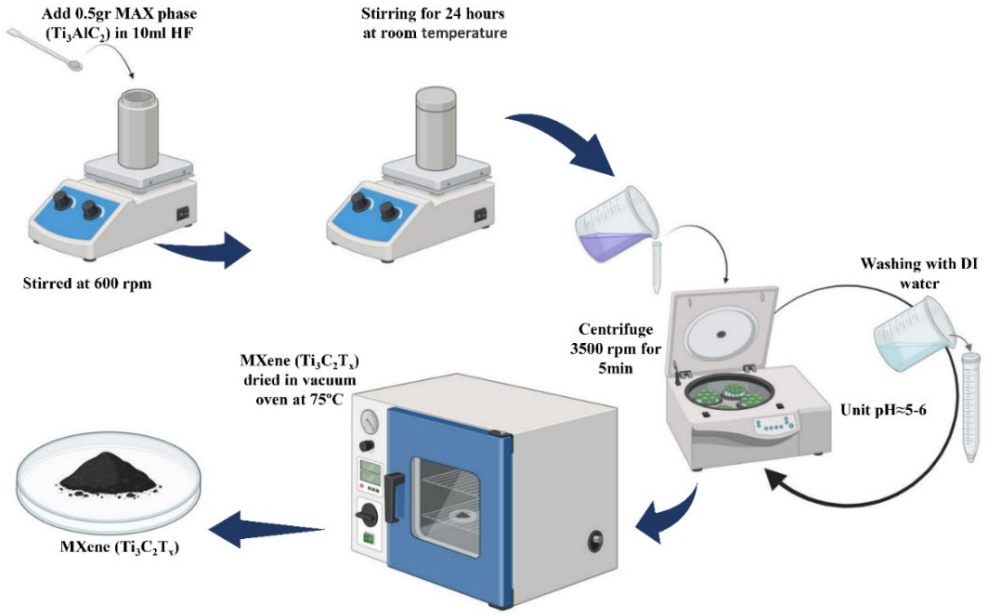

Figure 1. Schematic Diagram of the Process for Preparing $Ti_3C_2T_x$ MXene by Etching Ti_3AlC_2 with HF

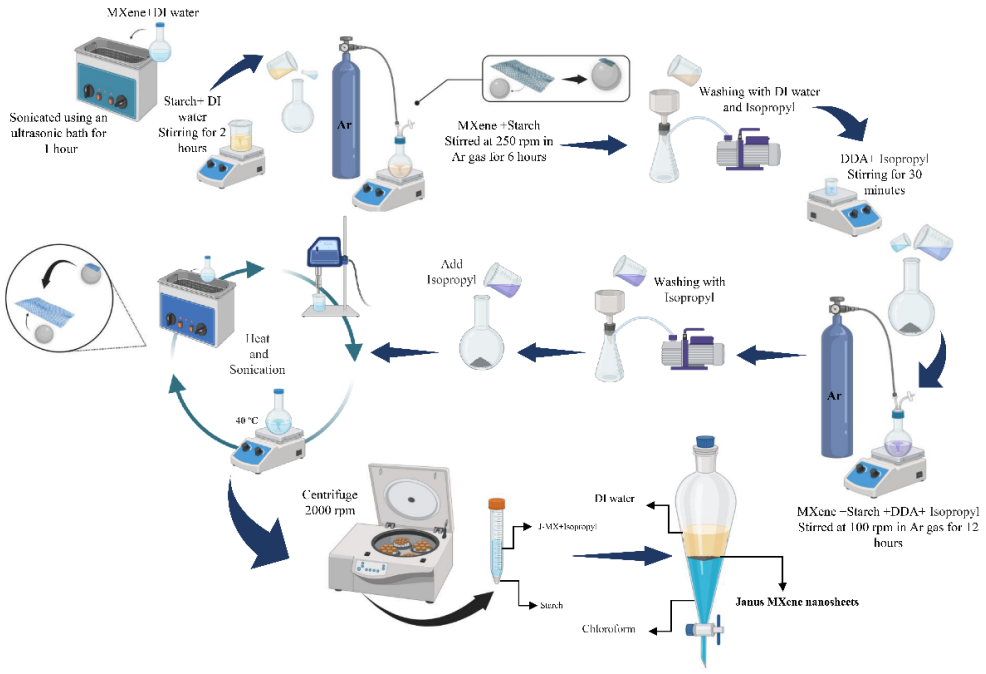

Figure 2. Schematic Diagram of the Process for Preparing Janus MXene by Masking Starch.

3. Results and discussion

To confirm the successful synthesis of Janus MXene nanosheets, several analyses are required. First, place the Janus nanosheets in a two-phase solution: a hydrophobic phase (chloroform) and a hydrophilic phase (DI water). As shown in Figure 3, the Janus MXene is at the interface between the two phases.

The second approach is to investigate the structure and morphology of MXene and Janus MXene using FESEM images. The image in Figure 4a illustrates an MXene-coated starch microsphere. Distinct and well-separated microspheres are visible, indicating that the MXene nanosheets have been successfully adsorbed onto the surface of the starch microspheres. Figure 4b shows that MXene was etched with HF (40%) to form multilayers stacked on top of one another via weak van der Waals interactions. Figure 4c shows the FESEM image of Janus MXene; which, due to delamination with DMSO, a two-dimensional structure with fewer layers is observed, confirming the successful synthesis of the two-dimensional nanosheets.

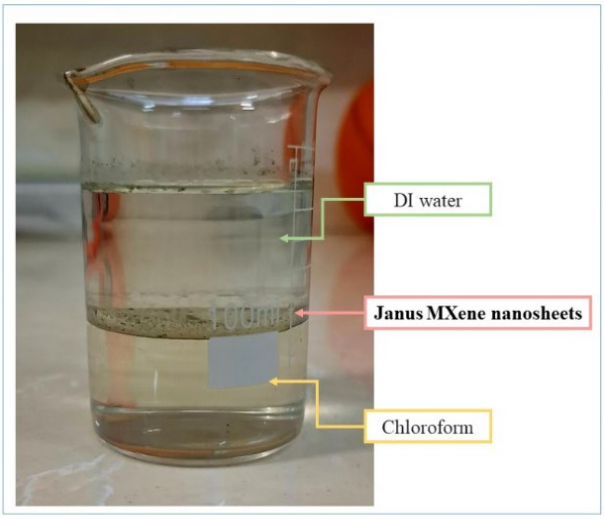

Figure 3. Janus MXene nanosheets between two-phase: hydrophilic and hydrophobic phases.

The third approach is an FTIR analysis of the dodecyl amide bonded to MXene. As shown in Figure 5, the FTIR spectrum of MXene shows bands at 3719 cm^{-1} (O-H stretching), 2928 cm^{-1} (C-H stretching), 1707 cm^{-1} (C=O stretching), and 607 cm^{-1} (Ti-C stretching), confirming etching of MXene from the MAX phase [34,35]. Peaks at 1562 cm^{-1} (N–H bending of amide) [19, 36] and 1398 cm^{-1} (C–N stretch of amide) [34] confirm amide-carbonyl bonds, supporting the successful synthesis of the Janus MXene. Peaks at 2927 and 2856 cm^{-1} correspond to C–H stretching vibrations (CH and CH_2), confirming the successful modification of MXene by DDA.

The fourth section analyzes the structural bonds of MXene and Janus MXene bonds via Raman spectroscopy. Figure 6 shows that the MXene has four peaks from 100 to 800 cm^{-1}. Peaks at 154 and 610.7 cm^{-1} are linked to the E2g mode of the carbon sublattice, while those at 257.5 and 428 cm^{-1} relate to E1g and A1g modes, representing in-plane Ti-C vibrations. The D and G bands at 1311 and 1578 cm^{-1} confirm the presence of graphitic carbon. After modifying MXene with DDA, the 154 cm^{-1} peak shifted to 150 cm^{-1} in Janus MXene, indicating in-plane Ti atomic vibrations. Similarly, the 257.5 cm^{-1} peak moved to 250.5 cm^{-1}, reflecting contributions from out-of-plane Ti–C vibrations and H atoms in $Ti_3C_2(OH)_2$ [38]. The 428 cm^{-1} peak shifted to 425.5 cm^{-1}, suggesting out-of-plane Ti–C vibrations and O atoms in $Ti_3C_2(OH)_2$ [39]. After modification, the D and G bands shifted to 1320 and 1581.5 cm^{-1}, indicating partial recovery of sp^2 hybridization through DDA anchoring [40]. These Raman spectra confirm that the DDA modification and the synthesis of Janus MXene were successful.

The final analysis is the XRD spectrum of MXene and Janus MXene. Figure 7 shows MXene diffraction peaks at 9.1°, 18.1°, 27.3°, and 60.74°, corresponding to the Ti_3C_2 (002), (004), (006), and (110) planes, respectively. This is consistent with previous studies [41,42]. For Janus MXene, the (002) peak shifts to 8.7°, indicating increased interlayer spacing [41]. Similarly, after DDA modification, the peaks at 18.1° and 27.3° shift to 17.9° and 26.7°, confirming interlayer expansion of Ti_3C_2. In addition to peak shifts, a noticeable reduction in peak intensity, particularly for the

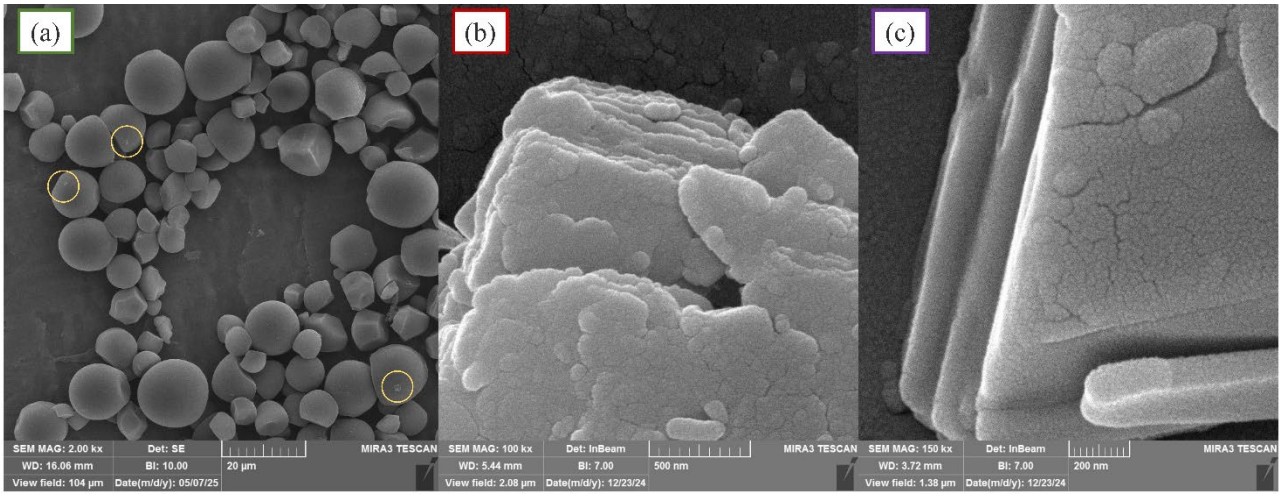

Figure 4. The FESEM images: a) MXene-coated starch microspheres, b) MXene, and c) Janus MXene nanosheet.

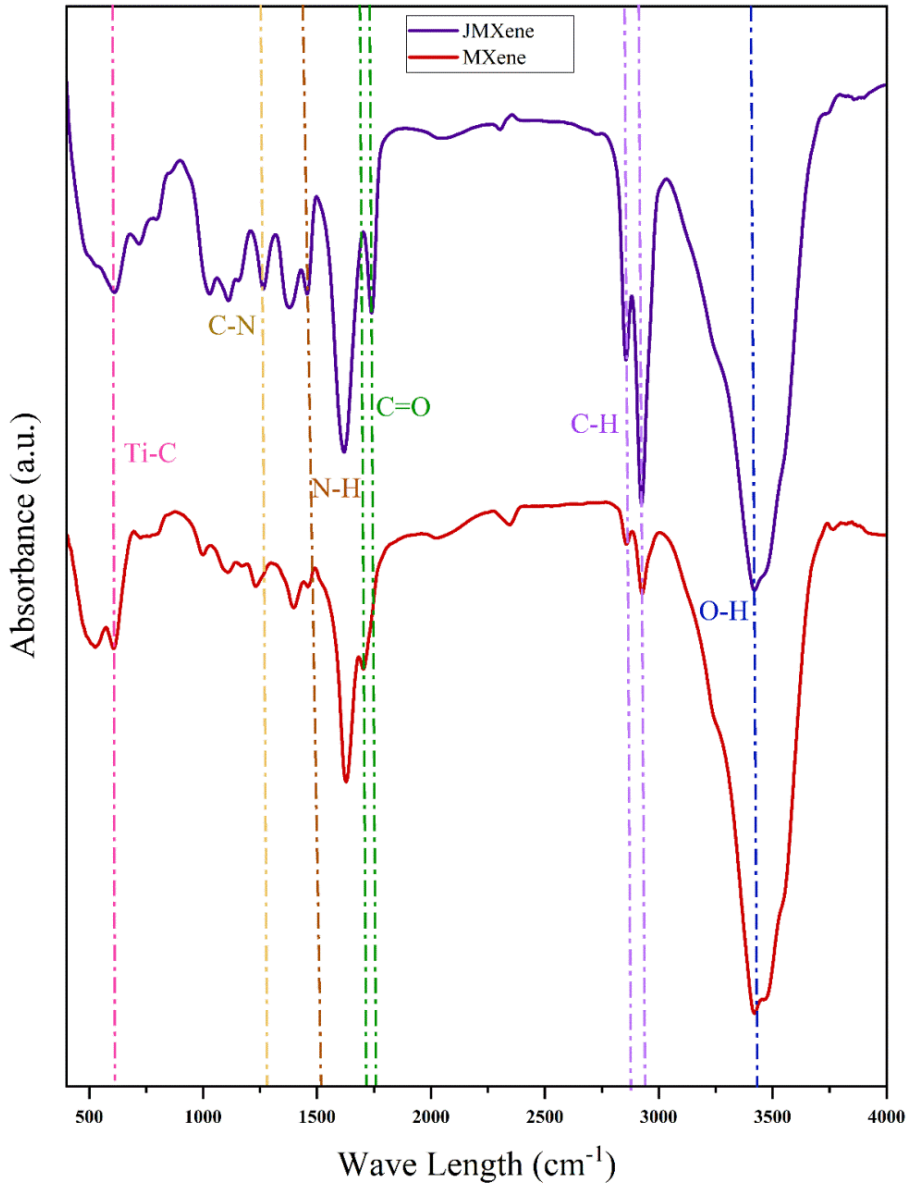

Figure 5. FTIR spectra of MXene and Janus MXene nanosheets.

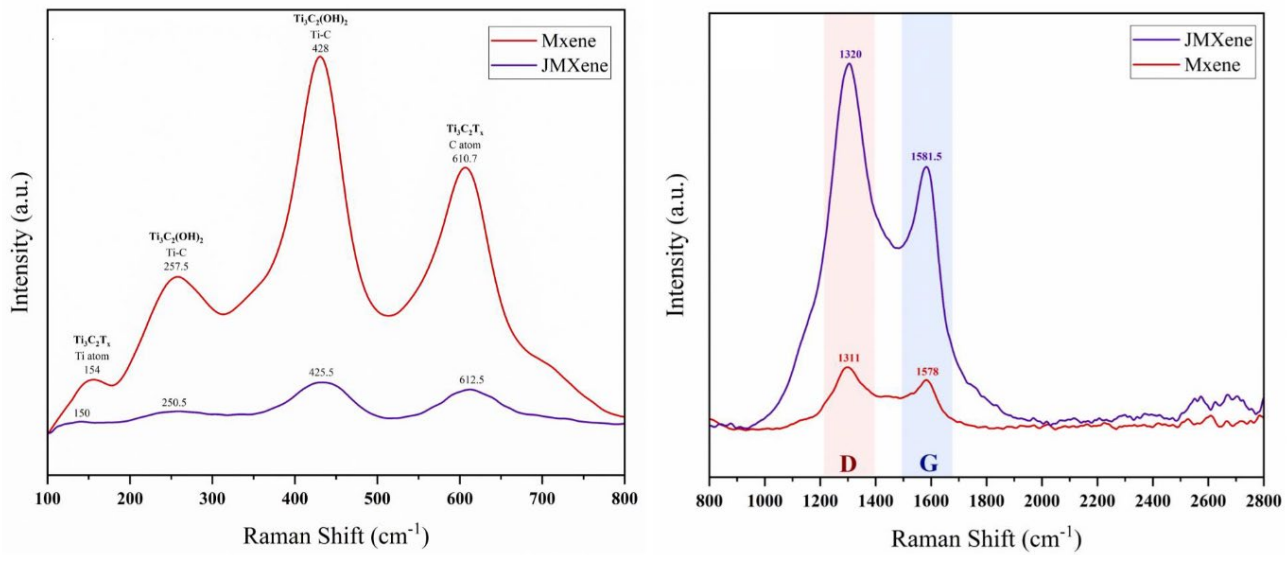

Figure 6. Raman spectra of MXene and Janus MXene nanosheets.

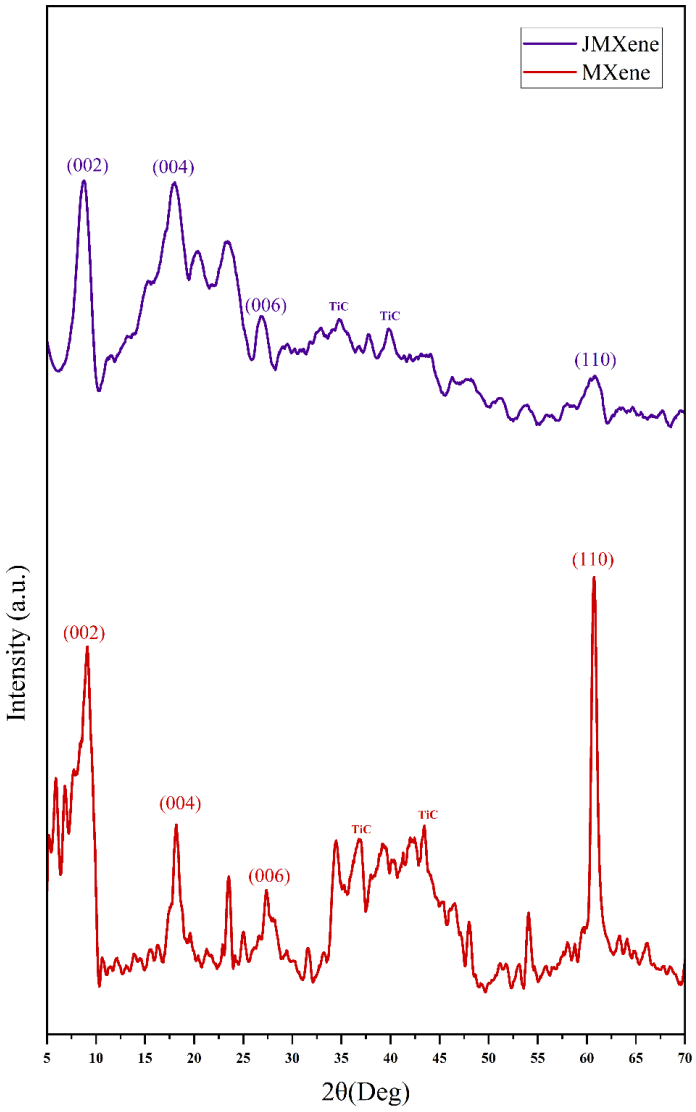

Figure 7. XRD spectrum of MXene and Janus MXene nanosheets.

(110) plane, is observed after modification. This decrease in intensity can be attributed to increased structural disorder, partial delamination, and reduced crystallinity resulting from interlayer expansion, as supported by the FESEM images. Moreover, the reduction in peak intensity may indicate partial oxidation of MXene during the modification process, as reported in the literature due to the sensitivity of Ti_3C_2 to oxygen and moisture. The absence of distinct TiO_2 peaks suggests that, if present, oxidation oxidation is limited to the surface. Overall, these XRD results confirm the successful formation of Janus MXene while highlighting the structural changes induced by DDA modification.

4. Conclusions

As discussed in this work, Janus MXene nanosheets were successfully synthesized using a low-cost and a simple masking strategy based on tapioca starch and DDA modification. Compared to previously reported approaches, this method avoids complex coating procedures and harsh thermal conditions, thereby reducing the risk of MXene structural degradation and oxidation. The asymmetric surface functionalization endows the Janus nanosheets with amphiphilic characteristics, making them promising candidates for engineering and environmental applications.

Nevertheless, several limitations should be acknowledged. The synthesis of MXene relies on HF-based etching of the MAX phase, which raises concerns regarding environmental safety, handling risks, and large-scale implementation. Although HF etching provides high-purity MXene with abundant surface functional groups, its corrosive nature necessitates strict safety protocols and limits industrial scalability. In addition, despite the use of the milder thermal conditions in the present approach, the partial oxidation and the long-term stability of Janus MXene under ambient conditions remain an important challenge that requires further investigation.

Future studies should therefore focus on developing safer and more environmentally benign etching routes, improving oxidation resistance, and systematically evaluating the scalability and durability of Janus MXene for practical applications.

References

1. Das R, editor. Two-Dimensional (2D) Nanomaterials in Separation Science. Springer International Publishing; 2021. https://doi.org/10.1007/978-3-030-72457-3
2. Kumar S, Kumari N, Seo Y. MXenes: Versatile 2D materials with tailored surface chemistry and diverse applications. J Energy Chem. 2024;90:253-293. https://doi.org/10.1016/j.jechem.2023.11.031
3. Panda S, Mehlawat S, Dhariwal N, et al. Investigation of Bi2MoO6/MXene nanostructured composites for photodegradation and advanced energy storage applications. Sci Rep. 2024;14:27416. https://doi.org/10.1038/s41598-024-78887-1
4. Ponce-Pérez R, Gutierrez-Ojeda SJ, Guerrero-Sánchez J, et al. A new family of copper-based MXenes. Sci Rep. 2021;11:12393. https://doi.org/10.1038/s41598-021-90628-2
5. Hakim ML, Alfarros Z, Herianto H, et al. High sensitivity flexible strain sensor for motion monitoring based on MWCNT@MXene and silicone rubber. Sci Rep. 2025;15:3741. https://doi.org/10.1038/s41598-025-88372-y
6. Alfalasi W, Hussain T, Tit N. Ab initio investigation of functionalization of titanium carbide Ti3C2 MXenes to tune the selective detection of lung cancer biomarkers. Sci Rep. 2024;14:1403. https://doi.org/10.1038/s41598-024-51692-6
7. Taherpoor P, Farzad F. Exploring the synergistic effect of MXene@ZIF-8 hybrid composites for water treatment. Sci Rep. 2025;15:11044. https://doi.org/10.1038/s41598-025-87527-1
8. Shi S, Qian B, Wu X, et al. Self-assembly of MXene-surfactants at liquid-liquid interfaces: from structured liquids to 3D aerogels. Angew Chem Int Ed Engl. 2019;58(50):18171-18176. https://doi.org/10.1002/anie.201908402
9. Montes-García V, Samorì P. Janus 2D materials via asymmetric molecular functionalization. Chem Sci. 2022;13(2):315-328. https://doi.org/10.1039/D1SC05836C
10. Azhdari S, Post Y, Trömer M, Coban D, Quintieri G, Gröschel AH. Janus nanoplates, bowls, and cups: controlling size and curvature via terpolymer/homopolymer blending in 3D confinement. Nanoscale. 2023;15(36):14896-14905. https://doi.org/10.1039/D3NR02902F
11. Pradhan S, Xu L, Chen S. Janus nanoparticles by interfacial engineering. Adv Funct Mater. 2007;17(14):2385-2392. https://doi.org/10.1002/adfm.200601034
12. Oake A, Bhatt P, Pathak YV. Understanding surface characteristics of nanoparticles. In: Surface Modification of Nanoparticles for Targeted Drug Delivery. 2019:1-17. https://doi.org/10.1007/978-3-030-06115-9_1
13. Li X, Chen L, Cui D, Jiang W, Han L, Niu N. Preparation and application of Janus nanoparticles: Recent development and prospects. Coord Chem Rev. 2022;454:214318. https://doi.org/10.1016/j.ccr.2021.214318
14. Wang S. A Research of Stereo-Selective Synthesis of Silica-based Amphiphilic Janus Particles. In: Journal of Physics: Conference Series. Vol 2133(1). IOP Publishing; 2021:012016. https://doi.org/10.1088/1742-6596/2133/1/012016
15. Bhat IM, Lone S. Hydrothermal and Laser-Guided Janus Membrane with Dual Wettability for Unidirectional Oil/Water Separation. ACS Appl Mater Interfaces. 2024;16(10):13225-13233. https://doi.org/10.1021/acsami.3c18059
16. Xie L, Jin W, Zuo X, Ji S, Nan W, Chen H, et al. Construction of small-sized superparamagnetic Janus nanoparticles and their application in cancer combined chemotherapy and magnetic hyperthermia. Biomater Sci. 2020;8(5):1431-1441. https://doi.org/10.1039/C9BM01880H
17. Meng X, Deng X, Zhou L, Hu B, Tan W, Zhou W, et al. A highly ordered hydrophilic-hydrophobic Janus bi-functional layer with ultralow Pt Loading and Fast Gas/Water Transport for Fuel Cells. Energy Environ Mater. 2021;4(1):126-133. https://doi.org/10.1002/eem2.12105
18. Chen M, Zhang Y, Li X, et al. Two-dimensional Janus MXene inks for versatile functional coatings on arbitrary substrates. ACS Appl Mater Interfaces. 2023;15(3):4591-4600. https://doi.org/10.1021/acsami.2c20930
19. Akbari M, Shariaty-Niassar M, Matsuura T, Ismail AF. Janus graphene oxide nanosheet: A promising additive for enhancement of polymeric membranes performance prepared via phase inversion. J Colloid Interface Sci. 2018;527:10-24. https://doi.org/10.1016/j.jcis.2018.05.012
20. Zhao S, Chen Y, Zhang H, et al. Janus MXene nanosheets for macroscopic assemblies. Mater Chem Front. 2020;4(3):910-917. https://doi.org/10.1039/C9QM00681H
21. Chen X, Li W, Fan Q, Liu X, Zhai X, Shi X, et al. Amphiphilic Janus Nanoparticles for Effective Treatment of Bacterial Pneumonia by Attenuating Inflammation and Targeted Bactericidal Capability. Int J Nanomedicine. 2024;19:12039-12051. https://doi.org/10.2147/IJN.S486450
22. Zhang S, Jiang T, Li M, Sun H, Wu H, Wu W, et al. Multifunctional wearable triboelectric nanogenerators prepared by combined crystallization and diffusion method: High-output, breathable, antimicrobial, and Janus-wettability for smart control and self-powered biosensing. Nano Energy. 2024;131:110214. https://doi.org/10.1016/j.nanoen.2024.110214
23. Dar GI, Iqbal MZ. Multifunctional biocompatible Janus nanostructures for biomedical applications. Curr Opin Biomed Eng. 2019;10:79-88. https://doi.org/10.1016/j.cobme.2019.04.001
24. Chen Y, Cao J, Li Y, Zeng H. Multiscale study of Janus nanosheets' interfacial activity. J Mol Liq. 2024;394:123740. https://doi.org/10.1016/j.molliq.2023.123740
25. Su H, Li S, Yang GZ, Qian K. Janus micro/nanorobots in biomedical applications. Adv Healthc Mater. 2023;12(16):2202391. https://doi.org/10.1002/adhm.202202391
26. Ou J, Wu B, Wang F, Xue M. Textile with Janus wetting properties via copper deposition and subsequent chemical vapor deposition of 1-dodecanethiol. Mater Lett. 2019;251:5-7. https://doi.org/10.1016/j.matlet.2019.04.105
27. Ng SW, Noor N, Zheng Z. Graphene-based two-dimensional Janus materials. NPG Asia Mater. 2018;10(4):217-237. https://doi.org/10.1038/s41427-018-0023-8
28. De Leon AC, Rodier BJ, Luo Q, Hemmingsen CM, Wei P, Abbasi K, et al. Distinct chemical and physical properties of Janus nanosheets. ACS Nano. 2017;11(7):7485-7493. https://doi.org/10.1021/acsnano.7b04020
29. Ge Y, Wang T, Zheng M, Jiang Z, Wang S. Controlled one-sided growth of Janus TiO2/MnO2 nanomotors. Nanotechnology. 2019;30(31):315702. https://doi.org/10.1088/1361-6528/ab19c7
30. Wang Y, Wang Y. Recent progress in MXene layers materials for supercapacitors: high-performance electrodes. SmartMat. 2023;4(1):e1130. https://doi.org/10.1002/smm2.1130
31. Mahmud ST, Hasan MM, Bain S, Rahman ST, Rhaman M, Hossain MM, et al. Multilayer MXene heterostructures and nanohybrids for multifunctional applications: a review. ACS Mater Lett. 2022;4(6):1174-1206. https://doi.org/10.1021/acsmaterialslett.2c00175
32. Zhang H, Fu ZH, Legut D, Germann TC, Zhang RF. Stacking stability and sliding mechanism in weakly bonded 2D transition metal carbides by van der Waals force. RSC Adv. 2017;7(88):55912-55919. https://doi.org/10.1039/C7RA11139H
33. Chavan RA, Ghule AV. Influence of binder and solvents on the electrochemical performance of screen-printed MXene electrodes. Nanotechnology. 2023;34(37):375401. https://doi.org/10.1088/1361-6528/acde85
34. Liu Z, Lv H, Xie Y, Wang J, Fan J, Sun B, et al. A 2D/2D/2D Ti3C2Tx@TiO2@MoS2 heterostructure as an ultrafast and high-sensitivity NO2 gas sensor at room-temperature. J Mater Chem A. 2022;10(22):11980-11989. https://doi.org/10.1039/D1TA09369J
35. Aparna R, Iyer RS, Das T, Sharma K, Sharma A, Srivastava A. Detection, discrimination and aging of human tears stains

using ATR-FTIR spectroscopy for forensic purposes. Forensic Sci Int Rep. 2022;6:100290. https://doi.org/10.1016/j.fsir.2022.100290
36. Kewate OJ, Punniyakoti S. The role of HCl/LiF concentrations in the minimally intensive layer delamination (MILD) approach for synthesis of Ti3C2Tx MXenes. Results Eng. 2025;26:108598. https://doi.org/10.2139/ssrn.5624104
37. Yoon Y, Le TA, Tiwari AP, Kim I, Barsoum MW, Lee H. Low temperature solution synthesis of reduced two dimensional Ti3C2 MXenes with paramagnetic behaviour. Nanoscale. 2018;10(47):22429-22438. https://doi.org/10.1039/C8NR06854B
38. Sarycheva A, Gogotsi Y. Raman spectroscopy analysis of the structure and surface chemistry of Ti3C2Tx MXene. In: MXenes. Jenny Stanford Publishing; 2023:333-355. https://doi.org/10.1201/9781003306511-16
39. Eshtiaghi M, Ghasemi S, Shamsipur M, et al. Ternary Poly(3,4-ethylenedioxythiophene) Polystyrene Sulfonate/Ti3C2Tx/Silver Nanowire Electrochemical Aptasensor for Bisphenol-A Detection. Colloids Surf A Physicochem Eng Asp. 2025;712:138416. https://doi.org/10.1016/j.colsurfa.2025.138416
40. Luo D, Wang F, Vu BV, Chen J, Bao J, Cai D, et al. Synthesis of graphene-based amphiphilic Janus nanosheets via manipulation of hydrogen bonding. Carbon. 2018;126:105-110. https://doi.org/10.1016/j.carbon.2017.09.102
41. Chavan RA, Ghule AV. Influence of binder and solvents on the electrochemical performance of screen-printed MXene electrodes. Nanotechnology. 2023;34(37):375401. https://doi.org/10.1088/1361-6528/acde85
42. Dixit P, Maiti T. A facile pot synthesis of (Ti3AlC2) MAX phase and its derived MXene (Ti3C2Tx). Ceram Int. 2022;48(24):36156-36165. https://doi.org/10.1016/j.ceramint.2022.08.172